LASER BEAM PROPAGATION ALONG A VERTICAL PATH THROUGH THE FREE CONVECTION FLOW OF ABSORBING MEDIUM IN THE GRAVITAYIONAL FIELD

A.N.Kucherov

N.E. Zhukovskii Central Aero-Hydrodymics Institute, Moscow
Received December, 1995

We present here a study of propagation of a plane vertically directed laser beam through a gravitationally convective flow of an absorbing medium. The optical beam is considered in the paraxial approximation of the wave theory. The gravitational convection of the medium is treated based on Boussinesq equation. The comparison between regimes of the strong (developed) convection and moderate (viscous) one is made. The profiles of intensity, velocity and temperature are demonstrated for bottom, middle and top sections of the absorbing medium volume under study. The effect of diffraction and thermal blooming on the laser beam propagating under transient moderate (viscous) free convection regime is investigated.

Natural gravitational convection in h o r i z o n t a l laser beams was examined theoretically (see Refs. 1–3) and experimentally (see Refs. 4–9). There are some experimental studies of free convection in v e r t i c a l beams in gases (see Refs.10, 11) and liquids (see Refs. 12–14). Approximate analytical solutions were considered in Ref. 15. Numerical solution for steady-state convection in vertical column of radiation was obtained in Ref. 16, whereas those with the consideration of thermal blooming in the geometric optics approximation can be found in Ref. 17. In this paper, we study nonstationary thermal blooming of vertical laser beam propagating through an absorbing medium under gravitational convection conditions based on the wave optics.

Small-scale perturbations of medium parameters resulting from absorption of radiation are considered. In this case the following Navier–Stokes equation in Boussinesq approximation are valid:

$$\mathrm{div}\mathbf{V} = 0; \tag{1a}$$

$$\frac{\mathrm{d}}{\mathrm{d}t}\mathbf{V} + \frac{1}{\rho}\nabla p = \mathbf{g}\beta(T - T_0) + \nu\Delta\mathbf{V};$$

$$\frac{\mathrm{d}}{\mathrm{d}t} = \frac{\partial}{\partial t} + (\mathbf{V}, \nabla); \quad \nabla = \mathbf{i}\frac{\partial}{\partial x} + \mathbf{j}\frac{\partial}{\partial y} + \mathbf{k}\frac{\partial}{\partial z}; \tag{1b}$$

$$\frac{\mathrm{d}}{\mathrm{d}t}T = \frac{\alpha I}{\rho_0 C_p} + \chi\Delta T; \quad \Delta = \frac{\partial^2}{\partial x^2} + \frac{\partial^2}{\partial y^2} + \frac{\partial^2}{\partial z^2}. \tag{1c}$$

Here t is time; $\mathbf{V}$, ρ, p, and T are the velocity, density, pressure and temperature of the medium, respectively; ν is the coefficient of kinematic viscosity, $\mathbf{g}$ is strength of gravitational field (g is the acceleration due to gravity); χ is the thermal diffusivity; α is the absorption coefficient of the medium for radiation with the intensity I; C_p is the specific heat capacity of the medium at constant pressure; β is the coefficient of thermal expansion (for gases $\beta = 1/T$), T_0 is the initial temperature of the medium.

Let us now normalize the transverse coordinate, x, to the initial beam radius r_0, the vertical coordinate y to the path length L, and the velocity components v and u to the values V_L and $U = V_L(r_0/L)$ (to be defined below). Besides, let us use time t normalized to the characteristic time of the gravitational convection development, $\tau = V_L/L = U/r_0$. Let also the temperature and pressure be normalized to T_0 and p_0, and the radiation intensity be normalized to the characteristic value $I_0 = W_0/\pi r_0^2$, where W_0 is the total initial power of the beam. With these designations, Eqs.(1) take the following form:

$$\mathrm{div}\mathbf{V} = 0; \quad T = 1 + QT_1 + \ldots;$$

$$p/p_0 = 1 + (\rho_0 gL/p_0)[(y_0 - y) + Qp_2 + \ldots]; \tag{2a}$$

$$\frac{\mathrm{d}}{\mathrm{d}t}\mathbf{V} = \frac{Q}{\mathrm{Fr}}(\mathbf{j}T_1 - \nabla p_2) + \frac{1}{\mathrm{Re}}\Delta'\mathbf{V};$$

$$\Delta' = \frac{\partial^2}{\partial x^2} + \frac{r_0^2}{L^2}\frac{\partial^2}{\partial y^2} + \frac{\partial^2}{\partial z^2}; \tag{2b}$$

$$\frac{\mathrm{d}}{\mathrm{d}t}T_1 = I + \frac{1}{\mathrm{Pe}}\Delta' T_1 \tag{2c}$$

Here $\mathrm{Re} = Ur_0/\nu = r_0^2 V_L/\nu L$ is Reynolds number; $\mathrm{Pe} = Ur_0/\chi = r_0^2 V_L/\chi L = \mathrm{Pr}\,\mathrm{Re}$ is Péclet number, $\mathrm{Pr} = \nu/\chi$ is Prandtl number, $\mathrm{Fr} = V_L^2/gL$ is Froud number; $Q = q_0 L/\rho_0 h_0 V_L \equiv \tau/\tau_q$ is the scale of the medium temperature (density) perturbations;

0235-6880/96/08 706-07 $02.00

$\tau_q = \rho_0 h_0 / q_0$ is the characteristic time of the medium temperature change being heated with a heat source of intensity $q_0 = \alpha I_0$; $h_0 = C_p T_0$ is the enthalpy of unperturbed medium. From the equation of the transverse momentum conservation (1b) it follows that pressure perturbation function p_2 in a narrow and extended beam ($r_0/L \ll 1$) depends only on vertical coordinate y with an error $O(r_0^2/L^2)$. If the side walls parallel to the beam are widely spaced, it is believed that $p_2 = 0$. Therefore, we neglect p_2 below. Notice that if we pass to current and vorticity functions, the pressure p can be in the general case canceled from Eq.(1b) since rot×grad $p = 0$.

The wave equation describing laser beam propagation in the paraxial approximation ($r_0/L \ll 1$) takes the form:

$$-2iF \frac{\partial f}{\partial y} + \Delta_\perp f = -(iN_\alpha F + 2F^2 N T_1) f, \qquad (3)$$

Here f is the complex amplitude of the electromagnetic field determining its intensity $I = f^* f$; $F = 2\pi r_0^2/\lambda L$ is the Fresnel number, λ is the radiation wavelength, $\Delta_\perp$ is the Laplacian with respect to transverse coordinates, i is the imaginary unit, $N_\alpha = \alpha L$ is the radiation absorption parameter of the medium, $N = (L/r_0^2) Q(-\partial O/\partial T\, T_0)/O_0$ is the thermal blooming parameter, O_0 is refraction index of unperturbed medium. Let us assume that the origin of coordinates is placed at the beam center and the volume of absorbing medium has a rectangular cross section of $L_x \times L_y$ size. Furthermore, it is assumed that along the direction of the coordinate axes normal to x and y axes the vessel is long enough for radiation distribution and medium flow to be considered plane. The initial radiation distribution at the entrance of the absorbing medium at $y = y_0 = -L/2$ (propagation occurs from bottom to top) is given by Gaussian form: $f_{y=y_0} = \exp(-x^2)$ for $t \geq 0$. Condition of the field decay at a long transverse distance is assumed to be of the form $f_{x \to \mp\infty} \to 0$.

The velocity V_L can be defined by two methods. By equalizing the Archimedes force in the right-hand side of Eq.(2*b*) to the inertial terms in its left-hand side ($Q/\mathrm{Fr} = 1$) one can obtain regime of s t r o n g or d e v e l o p e d convection described by the following expressions:

$$V_L = \left(\frac{C_0 g\beta T_0 L^2}{\rho_0 h_0}\right)^{1/3}; \quad Q = \left(\frac{C_0}{\rho_0 h_0}\right)^{1/3} \left(\frac{L}{g\beta T_0}\right)^{1/3};$$

$$\tau = \left(\frac{\rho_0 h_0 L}{C_0 g\beta T_0}\right)^{1/3}. \qquad (4)$$

The d e v e l o p e d convection occurs at $\mathrm{Re} \geq 1$ and it is described by the equation of discontinuity (2a) along with the set of two transfer equations, (2*b*) and (2*c*), with (Re, Pe ~ 1) or without (Re, Pe ≫ 1) the allowance for viscosity and heat conductivity. In this regime there are two similarity parameters in addition to the elongation one, r_0/L, namely, Reynolds number $\mathrm{Re} = (\mathrm{Gr})^{1/2}(r_0/L)^2$ (here $\mathrm{Gr} = g\beta T_0 Q L^3/\nu^2$ is Grashof number) and Prandtl number $\mathrm{Pr} = \nu/\chi$ (or Péclet number $\mathrm{Pe} = \mathrm{Pr\,Re}$).

At low Reynolds number $\mathrm{Re} \ll 1$, the last term in the right-hand side of Eq.(2b) describing friction stress counterbalances Archimedes force, whereas the inertial terms can be ignored. Taking Archimedes force equal to the friction stress, $Q\mathrm{Re} = \mathrm{Fr}$, one can obtain the following characteristic quantities for the m o d e r a t e v i s c o u s convection regime:

$$V_L = \left(\frac{C_0 g\beta T_0 L r_0^2}{\rho_0 h_0 \nu}\right)^{1/2}; \quad Q = \left(\frac{C_0 \nu L}{r_0^2 \rho_0 h_0 g\beta T_0}\right)^{1/2};$$

$$\tau = \frac{L}{V_L} = \left(\frac{\rho_0 h_0 L\nu}{C_0 g\beta T_0 r_0^2}\right)^{1/2}. \qquad (5)$$

Let us now consider the m o d e r a t e v i s c o u s convection regime in liquids with high Prandtl number $\mathrm{Pr} \gg 1$, such that Péclet number $\mathrm{Pe} = \mathrm{RePr} \gtrsim 1$. This situation was investigated experimentally for PES-1, PES-4, PMS-20 and PMS-1000 organosilicon liquids in Ref.12-14. Some numerical solutions for steady process are given in Ref.17. According to energy conservation equation (2c) the process characteristic time is τ, which is described by Eq.(5). Equation (2b) states that at any time $t \sim \tau$ the convection velocity is achieved in a shorter, "viscous," time $\tau_\nu = r_0^2/\nu \ll \tau$. Finally, we have the following set of equations instead of Eqs.(2):

$$\mathrm{div}\, \mathbf{V} = 0; \qquad (6a)$$

$$\Delta' v = -T_1; \qquad (6b)$$

$$\frac{\mathrm{d}}{\mathrm{d}t} T_1 = I + \frac{1}{\mathrm{Pe}} \Delta' T_1. \qquad (6c)$$

Parameter r_0/L and Péclet number $\mathrm{Pe} = U r_0/\chi = g\beta T_0 Q r_0^4/\nu\chi L \equiv \mathrm{Ra}(r_0/L)^4$, where $\mathrm{Ra} = g\beta T_0 Q L^3/\nu\chi$ is Reyleigh number (see Ref.18), are the similarity parameters of the problem. It can be shown that different Reynolds numbers, resulting from different characteristic velocities by Eqs.(4) and (5) for strong and moderate convection, are expressed through the same parameter, namely, heat complex A, used in Refs. 5 and 15:

$$\mathrm{Re}_{\mathrm{invisc}} = A^{1/3}; \quad \mathrm{Re}_{\mathrm{visc}} = A^{1/2}; \quad A = \frac{C_0 g\beta T_0 r_0^6}{\rho_0 h_0 L \nu^3}. \qquad (7)$$

Parameter A includes parameters that describe the beam and the medium. Condition $A \geq 1$ defines the regime of s t r o n g convection with low, moderate

and high heat conductivity in accordance with Prandtl number (or the substance of propagation medium), whereas condition $A \ll 1$ defines that for a moderate (viscous) convection.

Let us now use the functions of current, ψ, and vorticity, ω;

$$u = \frac{\partial \psi}{\partial y}; \quad v = \frac{\partial \psi}{\partial x};$$

$$\mathbf{\Omega} = \mathrm{rot}\mathbf{V} = (0, 0, \omega); \quad \omega = \left(\frac{\partial v}{\partial x} - \frac{\partial u}{\partial y}\right). \qquad (8)$$

The discontinuity equation turns into identity, whereas the relations of vorticity with the velocity components (8) give rise to Poisson equation for the current function ψ. The following set of equations for dimensionless functions ψ, ω, and T_1 can be derived from Eqs.(6) for the regime of moderate convection

$$\Delta' \psi = -\omega; \qquad (9a)$$

$$\Delta' \omega = -\frac{\partial}{\partial x} T_1; \qquad (9b)$$

$$\frac{\mathrm{d}}{\mathrm{d}t} T_1 = I + \frac{1}{\mathrm{Pe}} \Delta' T_1. \qquad (9c)$$

The set of equations for the regime of developed convection is similar to that presented in Ref.9. As to the horizontal laser beam (see Ref.9), evolution equation (9c) was solved by application of finite-differences McCormack scheme of the second order of approximation (see Ref.19). Poisson equations (9a) and (9b) along with paraxial ray equation (3) were solved using the expansion into Fourier series of the functions sought (see Refs. 20 and 21). In that case, terms with no less than second order were considered in the approximation. As to the velocities at the boundaries of a calculational region, we imposed here the conditions of sticking and leakage proof. The temperature at these boundaries was set to be of the initial value:

$$(u, v, T_1)|_{x = \mp Lx/2;\ y = \mp Ly/2} = 0. \qquad (10)$$

In our calculations, parameter $L = r_0$ was considered as a characteristic vertical size for normalizing. In this case, Laplacian in Poisson equations takes the common form: $\Delta = \partial^2/\partial x^2 + \partial^2/\partial y^2$. Besides, the inverse dimensionless path length (vessel height) $1/L_y$ becomes the nonproportionality (lengthening) parameter r_0/L. Another one similarity parameter, the Péclet number, characteristic time, velocity, and the scale of temperature rise become equal to:

$$\mathrm{Pe}' = \mathrm{Pe}(r_0/L)^{1/2}, \quad \tau' = \tau(r_0/L)^{1/2},$$

$$V_L' = V_L(r_0/L)^{1/2}, \quad Q' = Q(r_0/L)^{1/2}.$$

Similarity parameters in paraxial ray equation (3) are transformed as follows:

$$F' = F(L/r_0); \quad N_\alpha' = N_\alpha(r_0/L); \quad N' = N(r_0/L)^{5/2}.$$

Similarly, the following parameters can be obtained in the regime of developed convection with r_0 in place of the path length L:

$$\mathrm{Pe}' = \mathrm{Pe}(r_0/L)^{1/3}; \quad Q' = Q(r_0/L)^{1/3};$$

$$V_L' = V_L(r_0/L)^{2/3};$$

$$U' = U_L(r_0/L)^{5/3}, \quad \tau' = \tau(r_0/L)^{1/3}; \quad F' = F(L/r_0);$$

$$N_\alpha' = N_\alpha(r_0/L); \quad N' = N(r_0/L)^{7/3}.$$

The calculational results are presented in Figs. 1–4. Plots depicted in Figs. 1(*a* and *b*) allow high convection regime ($\mathrm{Re} \gtrsim 1$) to be related to the moderate one ($\mathrm{Re} \ll 1$) at the following similarity parameters: condition of thermal blooming $N = 3, 19$ and diffraction $F = 1.04$ of a beam. Both velocity components, u and v, are considerably higher for the developed convection regime (Fig. 1,*a*) as compared to those for the viscous one (Fig. 1,*b*). The velocity profile $v(x)$ is close in shape to the intensity distribution for the developed convection regime and becomes diffuse due to viscosity under moderate convection. Agitation in the convection regime gives a more smooth temperature profile and substantially reduces thermal blooming of the beam by the moment of quasi-established process, $t/\tau' = 20$, as compared to those in the transient flow at $t/\tau' = 4$ and 12. As illustrated by Fig. 2, an increase in the velocity and medium temperature at the initial time is evident in both regimes to be compared.

By the instant $t/\tau' = 4$, local perturbation peak is achieved in the middle and in the major part of the absorbing medium volume considered except for small regions in its lower and/or upper parts. Rate and amplitude of changes in velocity, medium density (temperature), beam intensity and beam average radius later significantly decrease, that is, slow quasi-establishment of the medium and beam parameters occurs. But at the given boundary conditions, in a limited, while reasonably large, volume $L_x \times L_y = 9.6 \times 9.6$ no complete establishment is achieved over extended periods $t/\tau' = 20 \div 40$.

The trends to slow temperature decrease under moderate (viscous) convection regime and velocity increase in a strong (developed) one are seen in Fig. 2. Both trends keep on in time. Quasi-establishment of the velocity and temperature with

deviations about several per cent of their average values are evident for moderate and developed convection regimes, respectively. For these regimes, temperature (density) perturbations at the symmetry axis $x = 0$ and at the initial time are peaking in the bottom part of the vessel. The peak of temperature perturbations in those regimes moves above one-half of the height of the vessel by $t/\tau' = 4$, and reaches its upper boundary by $t/\tau' \geq 8$ and then keeps maximum value under the regimes of strong and moderate convection (see Fig. 3). Similar variations of temperature profile with height are also evident in the case of thermally isolated upper boundary $(\partial T/\partial y)_{|y=L_y/2} = 0)$ of the vessel.

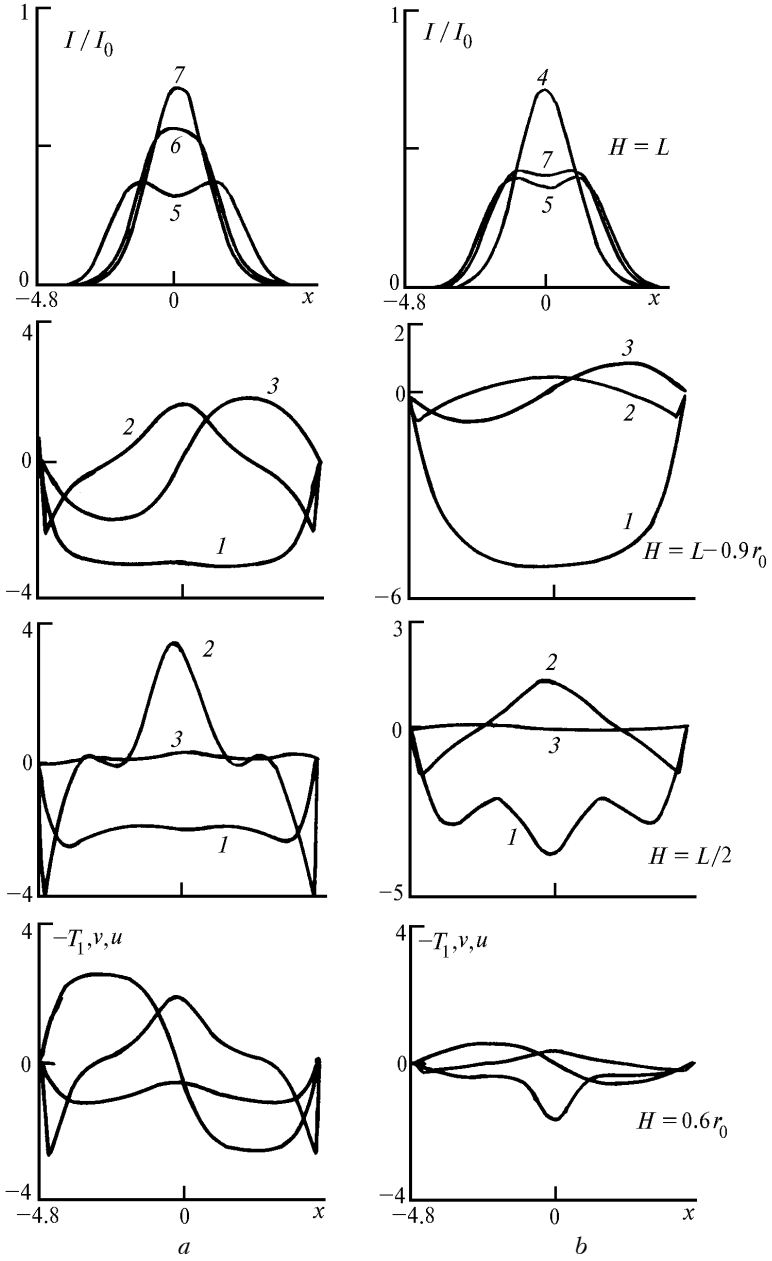

FIG. 1. Distribution of dimensionless temperature perturbations (curve 1) and velocity components $v = v_{ph}/V_L'$ *(curve 2),* $u = u_{ph}/U_L'$ *(curve 3) over transverse coordinate* x *at* $t/\tau' = 20$ *for strong (a) and moderate (b) convection at the bottom (height* $H = y - y_0 = 0.6r_0$*; the lower row of plots), at the center (*$H = L/2$*;* $y = 0$*; the second row) and at the top of the vessel under consideration (*$H = L - 0.9r_0$*;* $y = L/2 - 3\Delta y$*; the third row). Dimensionless beam intensity* $I(x)$ *at the end of the path (*$H = L$*;* $y = L_y/2$*) at:* $t/\tau' = 0$ *(curve 4), 4 (curve 5), 12 (curve 6), 20 (curve 7) is plotted in the upper row. The following similarity parameters were used:* $r_0/L = 0.104$; Pe = 15, F = 1.04; $N = 3.19$; $N_\alpha = 0.0104$; *along with a) Reynolds number* Re' = 20.8 (Pr = 0.72) *and b)* $\mathrm{Re} \ll 1$. *The calculational domain size and the number of grid nodes used are* $L_x = L_y = 9.6$, $N_x = 64$; $N_y = 32$.

Dynamics in the development of the convection velocities is qualitatively different in these two regimes. Under moderate convection, velocity peak is at the point lower than half height of the vessel at the initial time moment, and shifts higher ($y > 0$) by $t/\tau' = 4$ and then keeps its position near the height $H > L/2$ (see Fig. 3). Under developed convection, the peak of $v(y)$ is initially close to the bottom of the vessel, shifts to higher than one-half height (depending on parameters of the problem and, in particular, on the size of the vessel) later at $t/\tau' > 4$ and falls below middle the level $y = 0$ at $t/\tau' \geq 12$.

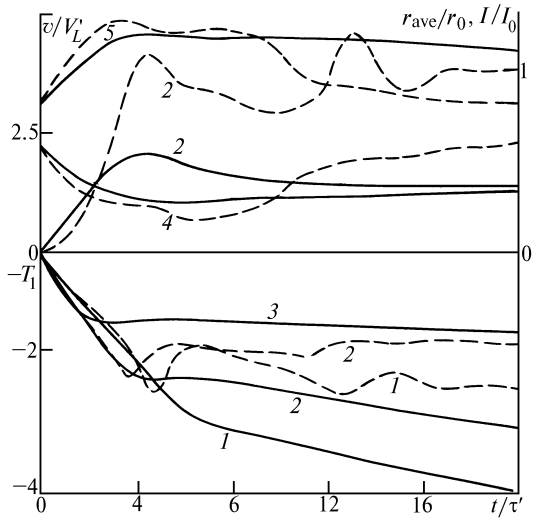

FIG. 2. Convection velocity v (curves 2), temperature T_1 (curves 1, 2, 3), intensity $I(x = 0)$ (curves 4) and average beam radius r_{ave} (curve 5) at the end of the path versus time for moderate convection (solid lines) and strong convection (dashed lines) regimes at the height of $H = 0.6r_0$ (1), $H = L/2$ (2), $H = L - 0.9r_0$ (3), $H = L$ (4, 5). Similarity parameters and parameters of calculation grid are identical to those in Fig. 1.

As indicated in Fig. 3 (dot-and-dash lines), increase in relative height of the vessel L/r_0 results in an increase of convection velocity in strong and moderate convection regimes and a comparative decrease of temperature perturbations under strong convection regime. Besides, the temperature is practically constant under moderate (viscous) convection regime. Distributions of the velocity ($v(y)$) and temperature ($T_1(y)$) with height weakly depend on an increase in L/r_0, other parameters being the same. Doubling of the vessel height results in the changes in the average beam radius, expressed as:

$$r_{ave}/r_0 = \sqrt{\int_{-\infty}^{\infty} x^2 I(x, y, t)\mathrm{d}x / W}$$

(here $W = \int_{-\infty}^{\infty} I(x, y, t)\mathrm{d}x$ is a dimensionless function of full power), by 0.5% and 5.9% under strong convection regime (see Fig. 1,*a*) and 9.5% and 7.8% under moderate convection (see Fig. 1,*b*) at $t/\tau' = 4$ and $t/\tau' = 20$, respectively.

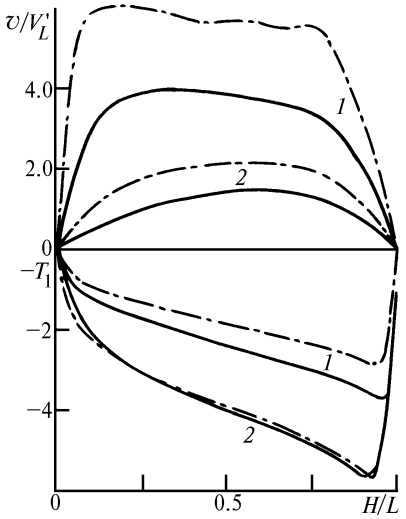

FIG. 3. Distribution of the velocity $v(x = 0)$ and temperature T_1 $(x = 0)$ with height in the case of strong (curves 1) and moderate (curves 2) convection at $t/\tau' = 20$. The following similarity parameters were used: Pe' = 15, $N = 3.19$, $N_\alpha = 0.0104$, $F = 1.04$ *(solid lines),* $r_0/L = 0.052$ *(dot-and-dash lines). The following calculation grid was used:* $L_x = 9.6$ ($N_x = 64$, $\Delta x = 0.15$), $L_y = 9.6$ ($N_y = 32$, $\Delta y = 0.3$ — *solid lines) and* 19.2 ($N_y = 32$, $\Delta y = 0.6$ — *dot-and-dash lines).*

Results of investigation of the beam perturbations under conditions of thermal blooming ranging from weak to strong ($N = 0$–3.19) for Fresnel number varying in the range of $F = 1 \div 7$ are presented in Figs. 4 *a*,*b*. The intensity of a plane Gaussian beam on the axis $x = 0$ changes in vacuum along the path $z \equiv H$ according to the following expression: $I/I_0 = 1/\sqrt{1 + (z/LF)^2}$. When $F \approx 1$, a decrease of the intensity by about 30% in vacuum and by more than 60% under moderate convection regime at self-refraction in free-convective flow is observed (see Fig. 1,*b*). If Fresnel number is in the range from 2 to 7 (see Fig. 4,*a*), a circular distribution of the intensity with a deep fall at its center instead of a bell-shaped distribution is observed as a result of thermal blooming. Circular peak of the intensity with the radius slightly exceeding the exponential one is observed at $F > 3$. The maximum difference between the intensity at the center of the fall and that on the circle is observed at $t/\tau' = 4$. If $F > 5$, intensity at the center, average beam radius and average intensity, $I_{ave}(y, t)/I_0 = Wr_0/r_{ave}\sqrt{\pi}$, do not change. When $F = 1$, the fall is slightly seen even at maximum perturbations of the medium and the beam ($t/\tau' \cong 4$) and at $F < 1$ it disappears at all.

Changes in the thermal blooming parameter N under conditions of diffraction blooming in the case of $F \approx 1$ normally provides extra blooming of the beam. As illustrated in Fig. 4, varying of N at a considerably high Fresnel number $F = 5 \div 7$ affects not only the intensity distribution shape, but the average parameters as well.

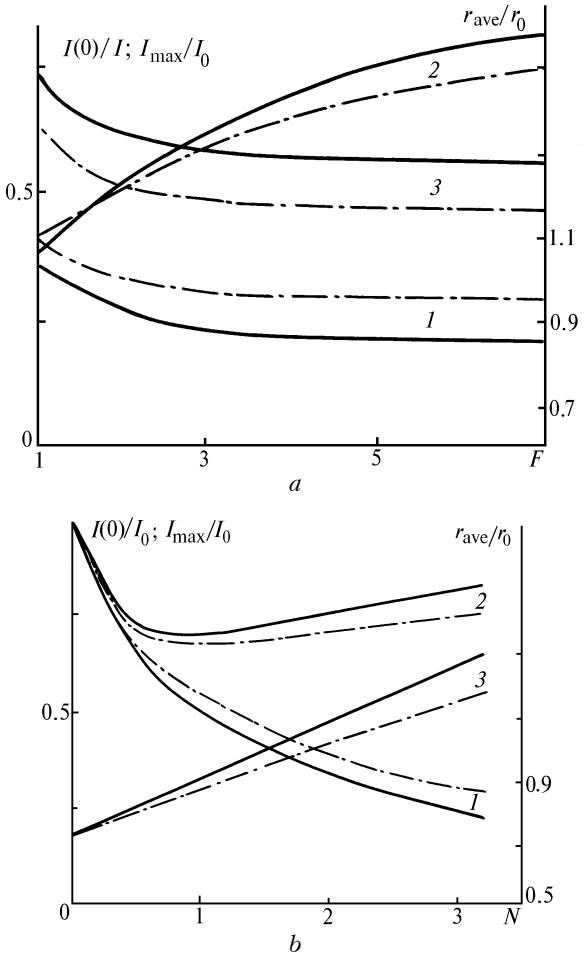

FIG. 4. Intensity at the center of the beam $I(x = 0)$ (curve 1), peak intensity I_{max} (curve 2) and average radius of the beam r_{ave} (curve 3) at the end of the path $H = L$ at $t/\tau' = 4$ (solid lines) and $t/\tau' = 20$ (dot-and-dash lines) versus Fresnel number at $N = 3.19$ (a) and thermal blooming parameter N at $F = 7$ (b). Calculation grid parameters were as follows: $N_x = 64$, $N_y = 32$, $\Delta x = 0.15$, $\Delta y = 0.3$, $L_x = L_y = 9.6$; $N_\alpha = 0$, Pe' = 15, $r_0/L = 0.104$.

Once N is as low as 0.25, a noticeable fall appears at the center of intensity distribution about several per cent develops and reaches more than 70% at $N = 3.19$. Note that average radius increases linearly with N in the range of N under study. Besides, in the case of the initially collimated beam (in the present paper) and low absorbing parameter ($N_\alpha \cong 0$), the parameter N is identical to the thermal blooming factor $B_2(z)$ (see Refs. 22, 23), which normally describes multifrequency beams of a variable radius. The data presented in Ref.24 demonstrate average radius of a horizontal beam to be linear with the factor $B_2(z)$ and, in particular, with the parameter N under conditions of gravitational convection. In this paper, similar linear dependence of $r_{ave}(N)$ in vertical laser beam is shown.

Thus, the following conclusions can be drawn from the above:

1. Free convection regime in a vertical laser beam is determined by the magnitude of the heat complex $A = \alpha_0 I_0 g\beta T_0 r_0^6/(\rho_0 h_0 \nu^3 L)$. Developed strong convection regime is realized at $A \gtrsim 1$ ($\mathrm{Re} = A^{1/3}$), whereas moderate (viscous) convection regime is achieved at $A \ll 1$ ($\mathrm{Re} = A^{1/2}$).

2. The elongation parameter r_0/L along with a) Reynolds number $\mathrm{Re} = (\mathrm{Gr})^{1/2}(r_0/L)^2$ and Prandtl number under strong convection regime and b) Pe'clet number proportional to Rayleigh number $\mathrm{Pe} \equiv \mathrm{Ra}(r_0/L)^4 = g\beta T_0 Q r_0^4/\nu\chi L$ under moderate convection regime are similarity Parameters.

3. The height Profiles of hydrodynamic quantities and the average beam radius at the end of the Path weakly vary as the relative height $L_y = L/r_0$ increases in the range from 9.6 to 19.2, other similarity Parameters being the same.

4. Thermal blooming of the beam Provides its initial bell-shaPed intensity distribution to be transformed into that with the fall at the center. Moreover, the fall becomes deePer as Fresnel number and the thermal blooming Parameter increase.

5. The average radius of the vertical laser beam under moderate (viscous) convection regime increases linearly with the thermal blooming Parameter N.

ACKNOWLEDGMENT

This work has been done under financial suPPort from the Russian Foundation for Fundamental Research (Project No. 95-01-00453).

REFERENCES

1. J.R. Whinnery, D.T. Miller, and F. Dabby, IEEE J. Quant. Electron. **QE-3**, No.9, 382–383 (1967).
2. D.F. Smith, *ibid*. **QE-5**, No.12, 600–607 (1969).
3. V.A. Petrishchev, N.M. Sheronova, and V.E. Yashin, Izv. Vyssh. Uchebn. Zaved., Ser. Radiofizika **18**, No. 7, 963–974 (1975).
4. L.R. Bisonnette, Appl. Opt. **12**, No.4, 719–728 (1973).
5. B.P. Gerasimov, V.M. Gordienko, and A.P. Sukhorukov, Zh. Tekh. Fiz. **45**, No.12, 2485–2493 (1975).
6. V.A. Petrishchev, L.V. Piskunova, V.I. Talanov, and R.E. Erm, Izv. Vyssh. Uchebn. Zaved., Ser. Radiofizika **24**, No.2, 161–171 (1981).
7. I.A. Chertkova and S.S. Chesnokov, Atm. Opt. **3**, No. 2, 108–113 (1990).

8. V.P. Lukin and B.V. Fortes, Atm. Opt. **3**, No. 12, 1182–1185 (1990).
9. A.N. Kucherov, Atmos. Oceanic Opt. **6**, No. 12, 864–868 (1993).
10. R.A. Chodzko and S.C. Lin, AIAA J. **9**, No.6, 1105–1112 (1971).
11. J.P. Shuster, W.O. Li, and W.J. McLean, AIAA Paper, No. 80–1522 *"AIAA 15th Thermophysics Conference,"* Snowmass, Colorado (1980).
12. V.I. Zuev, Zh. Tekh. Fiz. **56**, No. 2, 394–396 (1986).
13. V.I. Zuev, Inzh. Fiz. Zh. **51**, No. 4, 584–586 (1986).
14. A.S. Gurvich and V.I. Zuev, *"Experimental investigation of convection induced by powerful laser radiation"*, Preprint (1987), 40 pp.
15. A.N. Bogaturov, V.I. Zuev, and V.M. Ol'khov, Zh. Eksp. Teor. Fiz. **94**, No. 8, 152–165 (1988).
16. B.P. Gerasimov, V.M. Gordienko, I.S. Kalachinskaya, and A.P. Sukhorukov, *"Numerical investigation of photoabsorption convection within vertical cylindrical pipe,"* Preprint No.63 (1975).
17. A.E. Galitch, and V.A. Petrushchenkov, Inzh. Fiz. Zh. **66**, No.5, 547-555 (1994).
18. L.D. Landau and E.M. Lifshits, *Hydrodynamics* (Nauka, Moscow, 1986), 736 pp.
19. R. Peyret and T.D. Taylor, *Computational Methods for Fluid Flow* (Springer Verlag, New York, 1983).
20. J.A. Fleck, J.R. Morris, and M.D. Feit, Appl. Phys. **10**, No.2, 129–160 (1976).
21. V.I. Polezhaev, A.V. Bune, N.A. Verezub, et al. *Mathematical Simulations of Convective Heat-and-mass Exchange Based on Navier-Stokes Equation* (Nauka, Moscow, 1987), 271 pp.
22. A.N. Kucherov, N.K. Makashev, and E.V. Ustinov, Izv. Vyssh. Uchebn. Zaved. SSSR, ser. Radiofizika **34**, No. 5, 528–535 (1991).
23. A.N. Kucherov, N.K. Makashev, and E.V. Ustinov, *ibid.* **36**, No.2, 135–142 (1993).
24. A.N. Kucherov, N.K. Makashev, and E.V. Ustinov, Atmos. Oceanic Opt. **6**, No. 12. 873–876 (1993).